



ELSEVIER

Physica E 14 (2002) 215–218

PHYSICA E

www.elsevier.com/locate/physce

Subpicosecond photoinduced electron transfer from a conjugated polymer to SnO₂ semiconductor nanocrystals

Neil A. Anderson^a, Encai Hao^a, Xin Ai^a, Gary Hastings^b, Tianquan Lian^{a, *}^aDepartment of Chemistry, Emory University, 1515 Pierce Drive, Atlanta, GA 30322, USA^bDepartment of Physics and Astronomy, Georgia State University, Atlanta, GA 30303, USA

Abstract

Photoinduced electron transfer from the conjugated polymer poly[2-methoxy, 5-(2'-ethyl-hexyloxy)-p-phenylenevinylene] (MEH-PPV) to a SnO₂ nanoporous thin film was studied using ultrafast IR spectroscopy. The absorption signals observed using this technique correspond to electron transfer, minimizing signal contamination from other processes. The electron transfer from polymer to nanocrystal was found to occur on an 800 fs timescale. The fast and efficient charge separation is attributed to the large interface area and favorable energetics for transfer. Charge separation is long-lived, persisting for microseconds. © 2002 Elsevier Science B.V. All rights reserved.

Keywords: Conjugated polymer; Semiconductor nanoparticle; Electron transfer; Ultrafast spectroscopy

1. Introduction

Composites of inorganic semiconductor nanoparticles [1] with conjugated polymers [2] are attractive photovoltaic materials because they may be able to combine the unique properties of the two materials. Conjugated polymer/inorganic semiconductor nanoporous films have some appealing characteristics, especially in Grätzel-type solar cell applications, where a photoexcited sensitizer can be used to transfer charge to the semiconductor [3]. The spectra and energy levels of conjugated polymers are tunable through functionalization. Charged conjugated polymers can also transport charge, which may allow the replacement of liquid electrolyte with an entirely solid-state system. Recently, a composite device with

a nanoporous TiO₂ layer and MEH-PPV as both the sensitizer and hole transporter was reported [4]. Using a nanocrystalline film provides a large interface and allows the inorganic semiconductor to transport the electron to an electrode through the inorganic network. The large interface may be especially critical for polymer/nanoparticle composites, since the polymer/semiconductor contact is not well defined. The polymer chromophore repeats along the chain, so it is important that the excitation on a polymer chain is close enough to reach the interface before it decays. Conjugated polymers typically have exciton diffusion radii of 5–15 nm [5]. Some recent work suggests that exciton localization can occur very quickly in these molecules [6].

Although charge transfer in conjugated polymer/semiconductor composites has been demonstrated for several systems, very little work has been done to directly study the transfer dynamics. We demonstrated previously that photoinduced electron transfer in an MEH-PPV/TiO₂ composite was extremely fast

* Corresponding author. Tel.: +1-404-727-6649; fax: +1-404-727-6586.

E-mail address: tlian@emory.edu (T. Lian).

(<100 fs) [7]. The polymer excited state has higher energy than the TiO₂ conduction band, resulting energetically favorable electron transfer [8,9]. Here, we expand on our study of photoinduced charge transfer in a MEH-PPV/SnO₂ composite. The SnO₂ conduction band is lower than TiO₂ [9], so electron transfer from MEH-PPV to SnO₂ is also energetically favorable. The long-lived charge separation is confirmed using microsecond step-scan FTIR spectroscopy. We also demonstrate that the charge separation timescale is apparent when probing in the visible region, although it is contaminated by overlapping absorption spectra of several species.

2. Experiment

Colloidal SnO₂ was synthesized according to a published procedure [7,10]. Films had good homogeneity and transparency. Average particle size was ~10 nm for SnO₂ from SEM measurements. MEH-PPV was also prepared by a published procedure [11], treating monomers with potassium tert-butoxide in organic solvents. SnO₂/MEH-PPV films were then prepared by soaking the nanoporous films in a 1 mg/10 ml chloroform solution of MEH-PPV for several hours, then rinsing with chloroform.

Ultrafast experiments were carried out using a 400 or 532 nm pump–mid-IR probe transient absorption scheme. Some visible probe experiments were also performed. The excitation power was ~3 μJ. The pump and the probe beam sizes at the sample were 500 and 300 μm, respectively. Details of the experimental setup have been described previously [12]. The sample was constantly moved during data collection to excite a fresh area. The pulse shape at the sample is approximately Gaussian, with FWHM ~200 fs. Microsecond step scan FTIR measurements were performed using a setup described elsewhere [13]. For these experiments, ~3 mJ of 532 nm light at 10 Hz with a ~8 mm beam size was used as the excitation source.

3. Results

Ultrafast kinetic traces were collected for MEH-PPV/SnO₂ film pumping at 400 nm, and probing

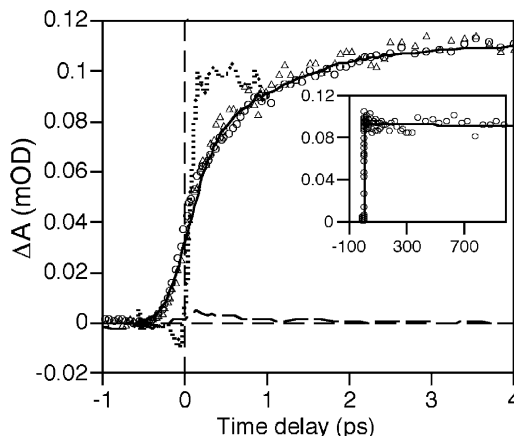


Fig. 1. The kinetic trace for MEH-PPV/SnO₂ using 400 nm excitation and 2000 cm⁻¹ probe is given by the open circles. Open triangles are the normalized trace with 530 nm excitation. The dashed line is the signal from a noninjecting MEH-PPV/ZrO₂ composite. The dotted line represents an instrument-limited rise, taken from the signal in a silicon wafer.

at probe energies ranging from 2550–1725 cm⁻¹. The dynamics of all IR-probe traces were identical within error. The two pump wavelengths resulted in identical dynamics. The IR signal arises entirely due to excitation of the polymer, since the excitation energy is well below the SnO₂ band gap. A naked SnO₂ film showed negligible signal. Fig. 1 shows the 2000 cm⁻¹ MEH-PPV/SnO₂ trace. The inset to Fig. 1 shows this trace extending to 1 ns. Traces from all probe wavelengths were globally fit by convoluting a Gaussian instrument function with a single exponential risetime (800 ± 200 fs) and a long-lived decay component (not clearly resolved). Very little (<10%) decay of the initial absorption signal was observed within 1 ns.

The mid-IR signal arises from photoinduced electron transfer from conjugated polymer to the semiconductor film. This transfer occurs when a polymer excitation (exciton) dissociates at the interface, leaving a hole on the polymer (positive polaron) and injecting an electron into the nanoparticle. The MEH-PPV positive polaron has a broad electronic absorption peaking at ~4300 cm⁻¹ [14]. Electrons injected into a semiconductor conduction band also exhibit very broad mid-IR absorption. The partitioning of the transient absorption signal between these species is not yet clear, although there is evidence that

the injected electron may dominate the absorption at the wavelengths studied [7]. Nevertheless, in the absence of other contributors, the 800 fs risetime of the mid-IR absorption corresponds to the photoinduced electron transfer in the MEH-PPV/SnO₂ composite.

Other species formed by excitation of the polymer can be shown to produce little contribution to the mid-IR signal. Polymer excitations may be localized on a single polymer chain (forming an exciton), or on adjacent chains (forming a polaron pair). Excitons are formed directly by excitation of the polymer. However, no instantaneous absorption is resolved in the trace. Furthermore, MEH-PPV excitons have a 200–300 ps lifetime at room temperature [15], while the composite signal shows very little decay within 1 ns. The observed trace is also not consistent with interchain charge transfer. Interchain charge transfer is strongly inhibited when polymer chains are dispersed [16], as in composites with nanoparticles. Additionally, interchain charge transfer also occurs very rapidly (< 100 fs) for MEH-PPV [17]. As a control experiment, a sample of MEH-PPV on nanoporous ZrO₂ was studied and the kinetic trace is shown in Fig. 1. ZrO₂ was chosen because electron transfer is energetically unfavorable from the photoexcited polymer to the nanoparticle conduction band [14]. The MEH-PPV/ZrO₂ signal size is negligible compared with MEH-PPV/SnO₂, supporting the assertion that the MEH-PPV/SnO₂ signal is predominantly due to electron transfer from polymer to nanoparticle.

Microsecond step-scan FTIR was used to verify photoinduced charge separation. A spectrum of MEH-PPV/SnO₂ is shown in Fig. 2. The sample exhibits two extremely broad absorption bands, and a narrower band at $\sim 1500\text{ cm}^{-1}$. The higher-energy band has a shallow peak at $4000\text{--}4500\text{ cm}^{-1}$, and coincides with the MEH-PPV polaron subgap absorption [14]. The narrow peak at 1500 cm^{-1} also arises from the charged polymer, and has been previously observed following photoinduced electron transfer from MEH-PPV to C₆₀ [18]. The lower-energy broad band is consistent with assignment to electrons injected into SnO₂ [7]. This spectrum indicates that charge separation has occurred. The kinetic trace is shown in the inset. It can be fit using a stretched exponential function with characteristic time $2.5\text{ }\mu\text{s}$ and distribution factor 0.29. All three absorption bands show identical dynamics in the step-scan data,

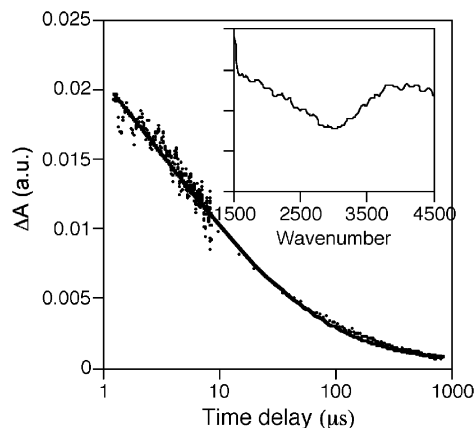


Fig. 2. Kinetic trace of electron signal from step-scan FTIR. The inset shows the spectrum of MEH-PPV/SnO₂ at $50\text{ }\mu\text{s}$. The $\sim 4000\text{ cm}^{-1}$ peak is from the MEH-PPV positive polaron. The broad band at lower energy comes from electrons injected into SnO₂.

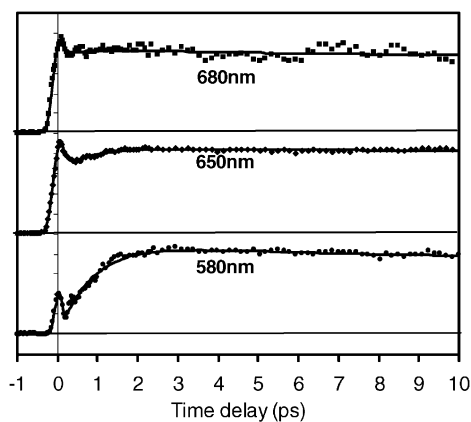


Fig. 3. MEH-PPV/SnO₂ kinetic traces, exciting at 400 nm and probing at the indicated wavelengths.

indicating that the microsecond decay comes from carrier recombination, rather than electron trapping in the film.

Visible probe data were also collected at several wavelengths. Fig. 3 shows traces for MEH-PPV/SnO₂ probing at 580, 650, and 680 nm. In addition to a spike, all the visible traces exhibit instantaneous absorption. A further absorption increase is also evident, especially at 580 nm. This component is well fit using an 800 fs exponential rise, in agreement with the mid-IR probe traces. However, complete analysis

of the visible probe traces is more difficult, since the visible probe signal also contains contributions not related to charge injection.

The results presented here indicate that charge transfer can be quite fast, and therefore efficient in polymer/nanoporous semiconductor film composites. We observed no direct evidence for slow exciton diffusion to the interface, which would cause delayed transfer. The MEH-PPV exciton diffusion radius is 10–20 nm, and the exciton decays on a ~ 300 ps timescale, so any slow injection should still occur within the 1 ns time window. The MEH-PPV/SnO₂ mid-IR signal shows a slight decay over a 1 ns timescale. It is possible that signal arising from slow injection could be masked by decay of the initial injected electron signal due to trapping or recombination. The observation of ultrafast charge injection can be partially attributed to the large interface presented by the nanoporous film. Additionally, the effective chromophore in conjugated polymers extends over several repeat units [19], which further facilitates electron transfer by increasing the probability that the excitation will be in contact with the interface. Finally, excitations in polymers have been shown to rapidly transfer energy to defect sites [6]. Ultrafast migration to the interface may thereby result from the communication between polymer segments, eliminating the need for slower migration.

The faster (< 100 fs) transfer from polymer to TiO₂ from Ref. [7] than to SnO₂ despite the lower energy of the SnO₂ conduction band is notable. Slower injection into SnO₂ than TiO₂ has been previously observed for semiconductor nanoparticles sensitized by molecular dyes, such as Ru N3 [Ru(II)(dcbpy)2(NCS)2 (dcbpy = 2,2'-bipyridyl-4,4'-dicarboxylato)] [20]. The SnO₂ conduction band consists of empty Sn⁴⁺ 5s orbitals, while the TiO₂ conduction band consists of empty Ti⁴⁺ 3d orbitals. We hypothesized that the π symmetry electron donating orbitals in Ru N3 have more favorable electronic coupling with π symmetry 3d orbitals in TiO₂ than 5s orbitals in SnO₂. Additionally, the effective mass of electrons in TiO₂ are $\sim 10m_e$, and only $\sim 0.3m_e$ in SnO₂ [21]. Although injection occurs higher in the conduction band for SnO₂, the density of states at the injection energy is lower than TiO₂. These two factors lead to a higher

electron injection rate from Ru N3 to TiO₂ than SnO₂ according to non-adiabatic interfacial electron transfer theory. Similar factors may be responsible for the faster electron transfer rate from conjugated polymer to TiO₂ than SnO₂. Work is ongoing to better understand the factors controlling the electron transfer rate.

Acknowledgements

This work is supported by a NSF CAREER award under grant CHE-9733796.

References

- [1] A.P. Alivasatos, *Science* 271 (1996) 933.
- [2] N.C. Greenham, R.H. Friend, *Solid State Phys.* 49 (1995) 1.
- [3] B. O'Regan, M. Grätzel, *Nature* 335 (1991) 737.
- [4] A.C. Arango, S.A. Carter, *Appl. Phys. Lett.* 74 (1999) 1698.
- [5] J.J.M. Halls, K. Pichler, R.H. Friend, S.C. Moratti, A.B. Holmes, *Appl. Phys. Lett.* 68 (1996) 3120.
- [6] D.A. Vanden Bout, W.-T. Yip, D. Hu, D.-K. Fu, T.M. Swager, P.F. Barbara, *Science* 277 (1997) 1074.
- [7] N.A. Anderson, E. Hao, X. Ai, G. Hastings, T. Lian, *Chem. Phys. Lett.* 348 (2001) 304.
- [8] M.M. Richter, F.R.F. Fan, F. Klavetter, A.J. Heeger, *Chem. Phys. Lett.* 226 (1994) 115.
- [9] A. Hagfeldt, M. Grätzel, *Chem. Rev.* 95 (1995) 49.
- [10] T. Nutz, U.Z. Felde, M. Haase, *J. Chem. Phys.* 110 (1999) 12 142.
- [11] C.J. Neef, J.P. Ferraris, *Macromolecules* 33 (2000) 2311.
- [12] Y.Q. Wang, J.B. Asbury, T. Lian, *J. Phys. Chem. B* 104 (2000) 4291.
- [13] G. Hastings, *Appl. Spectrosc.* 55 (2001) 894.
- [14] P.A. van Hal, M.P.T. Christiaans, M.M. Wienk, J.M. Kroon, R.A.J. Janssen, *J. Phys. Chem. B* 103 (1999) 4352.
- [15] L. Smilowitz, A. Hays, A.J. Heeger, G. Wang, J.E. Bowers, *J. Chem. Phys.* 98 (1993) 6504.
- [16] M. Yan, L.J. Rothberg, E.W. Kwock, T.M. Miller, *Phys. Rev. Lett.* 75 (1995) 1992.
- [17] D. Moses, A. Dogariu, A.J. Heeger, *Phys. Rev. B* 61 (2000) 9373.
- [18] U. Mizrahi, I. Shtrichman, D. Gershoni, E. Ehrenfreund, Z.V. Vardeny, *Synth. Methods* 102 (1999) 1182.
- [19] H.S. Woo, O. Lhost, S.C. Graham, D.D.C. Bradley, R.H. Friend, C. Quattrocchi, J.L. Bredas, R. Schenk, M.K., *Synth. Methods* 59 (1993) 13.
- [20] J.B. Asbury, E. Hao, Y.Q. Wang, H.N. Ghosh, T. Lian, *J. Phys. Chem. B* 105 (2001) 4545.
- [21] B. Enright, D. Fitzmaurice, *J. Phys. Chem.* 100 (1996) 1027.